Electronic Supplementary Material for CrystEngComm
This journal is (c) The Royal Society of Chemistry 2014

Supporting Information

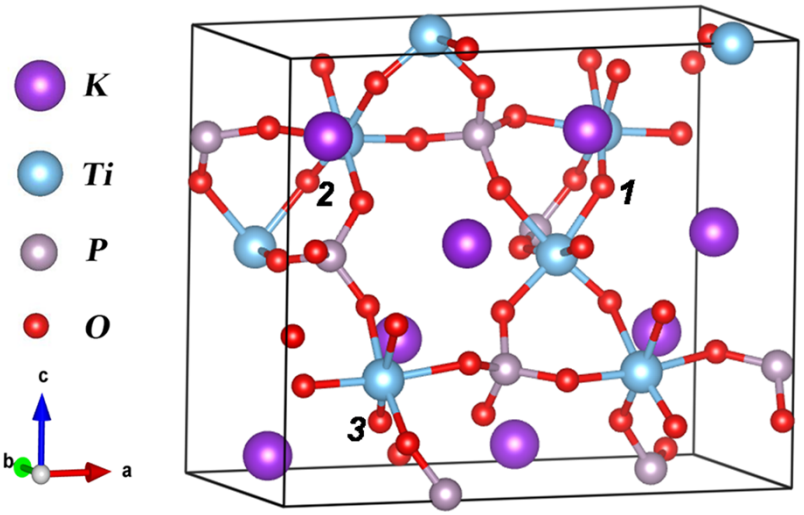

Fig. S1 View of KTP structure along *b*-axis. Numerals 1, 2 and 3 represent three different types of oxygen ions from O(Ti1)+O(Ti2). We consider conditions with different oxygen vacancy concentrations: one oxygen vacancy, two oxygen vacancies and three oxygen vacancies in one unit cell that are removed from a.) O ion 1, b.) O ions 1 and 2, c.) O ions 1, 2 and 3.

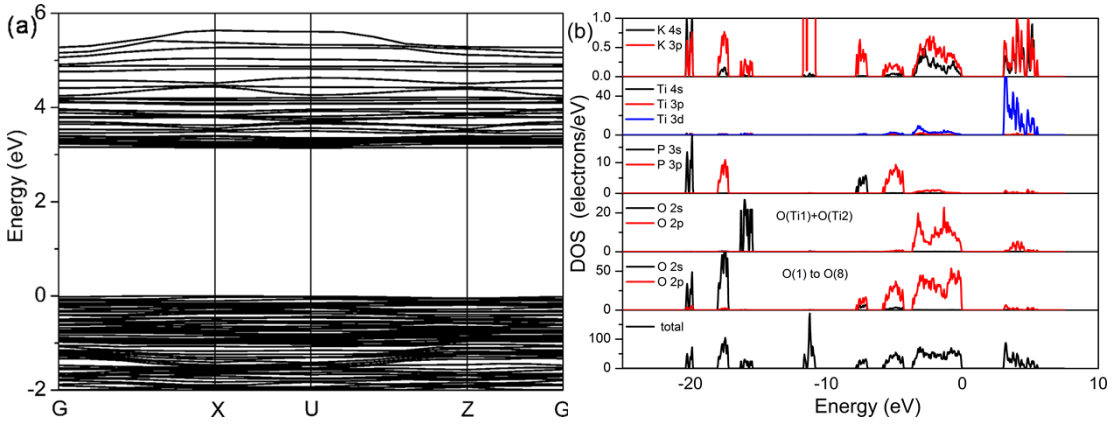

Fig. S2 (a) energy band structure, and (b) total density of states (TDOS) and partial density of states (PDOS) in KTP with one oxygen vacancy from O(Ti1)+O(Ti2) in a unit cell.

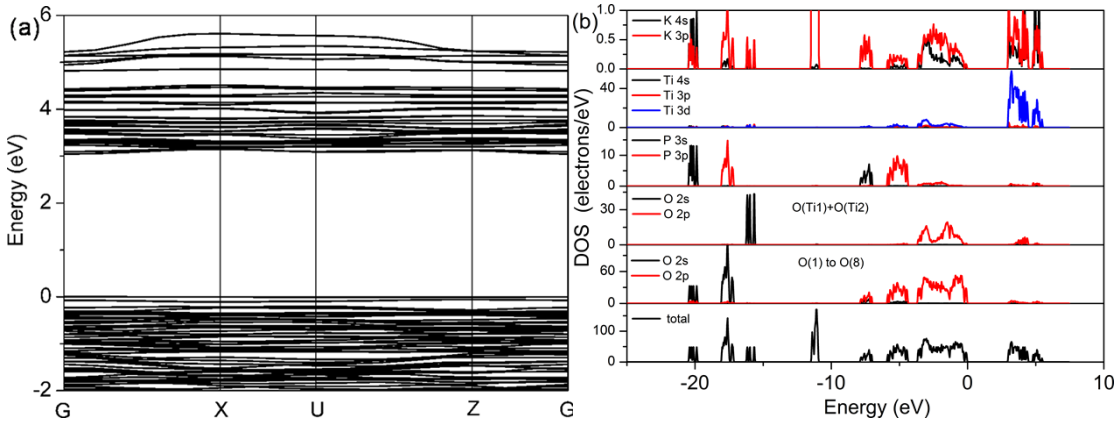

Fig. S3 (a) energy band structure and (b) total density of states (TDOS) and partial density of states (PDOS) in KTP with two oxygen vacancies from O(Ti1)+O(Ti2) in a unit cell.

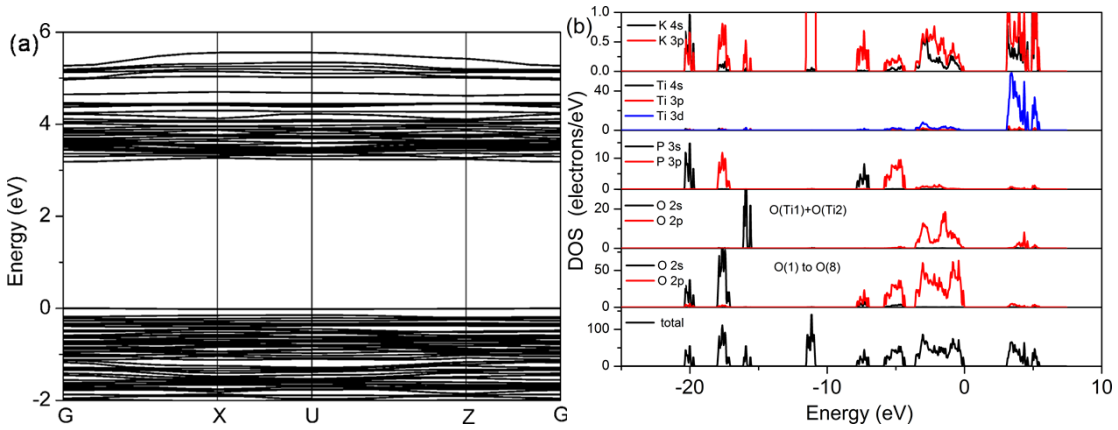

Fig. S4 (a) energy band structure and (b) total density of states (TDOS) and partial density of states (PDOS) in KTP with three oxygen vacancies from O(Ti1)+O(Ti2) in a unit cell.

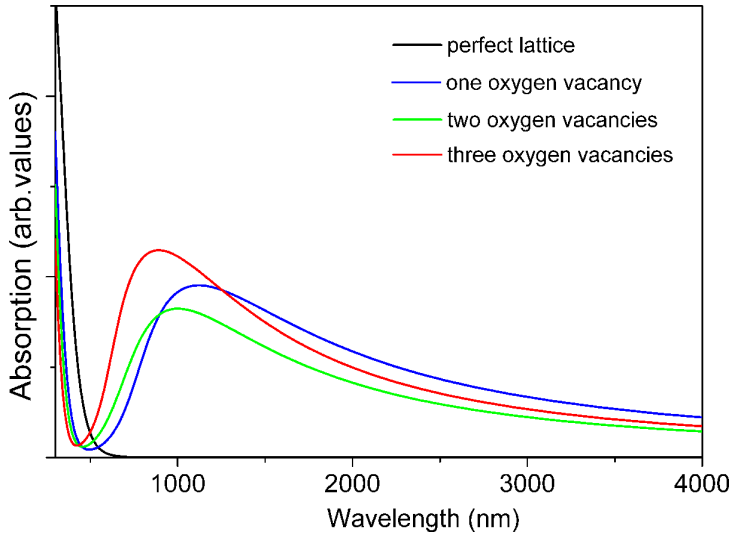

Fig. S5 Calculated absorption spectra of KTP with different oxygen vacancy concentrations from O(Ti1)-O(Ti2).

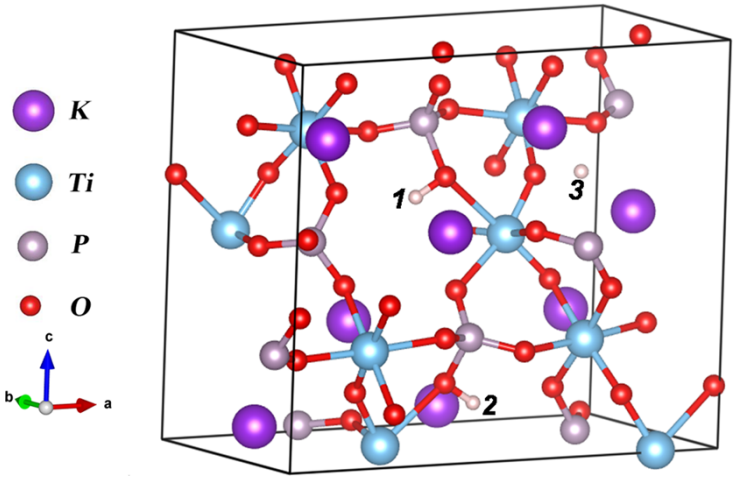

Fig. S6 View of KTP structure along *b*-axis. Numerals 1, 2 and 3 represent three different hydrogen ions bonding with O(1)-O(8). We consider the conditions of adding different concentrations of hydrogen ions bonding with O(1)-O(8): a.) one hydrogen ion 1, b.) two hydrogen ions 1 and 2, c.) three hydrogen ions 1, 2 and 3 in one unit cell bonded with oxygen ions.

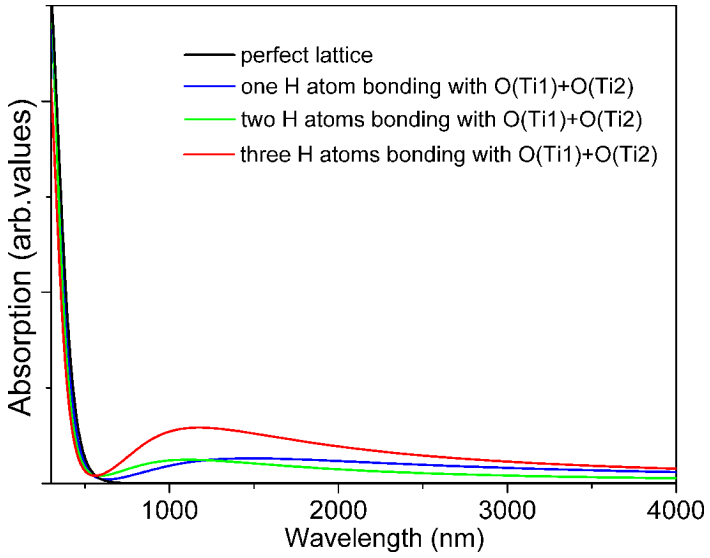

Fig. S7 Calculated absorption spectra of KTP by adding different concentrations of hydrogen atoms bonding with O(1)-O(8).

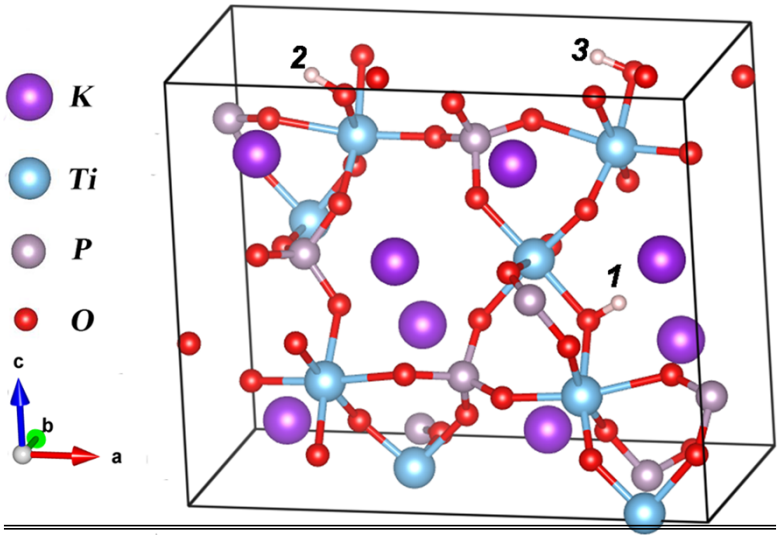

Fig. S8 Numerals 1, 2 and 3 represent three different hydrogen ions bonding with O(Ti1)-O(Ti2). We consider conditions by adding different concentrations of hydrogen ions bonding with O(Ti1)-O(Ti2): a.) one hydrogen ion 1, b.) two hydrogen ions 1 and 2, c.) three hydrogen ions 1, 2 and 3 in one unit cell bonded with oxygen ions.

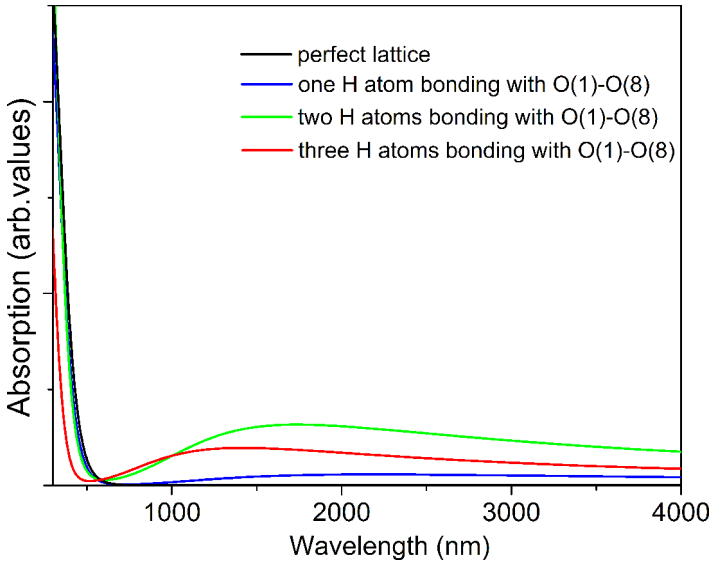

Fig. S9 Calculated absorption spectra by adding different concentrations of hydrogen ions bonding with O(Ti1)-O(Ti2).

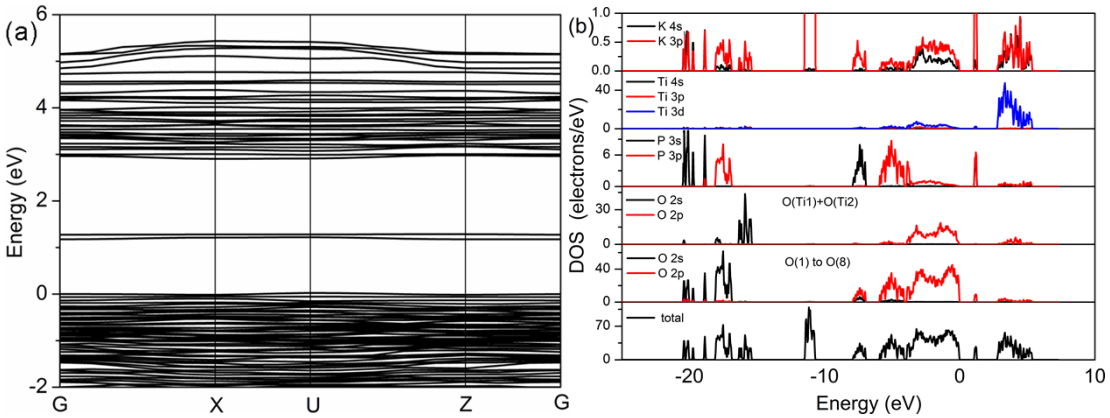

Fig. S10 (a) energy band structure and (b) the total density of states (TDOS) and partial density of states (PDOS) in KTP with two oxygen vacancies from O(1) to O(8) in a unit cell.

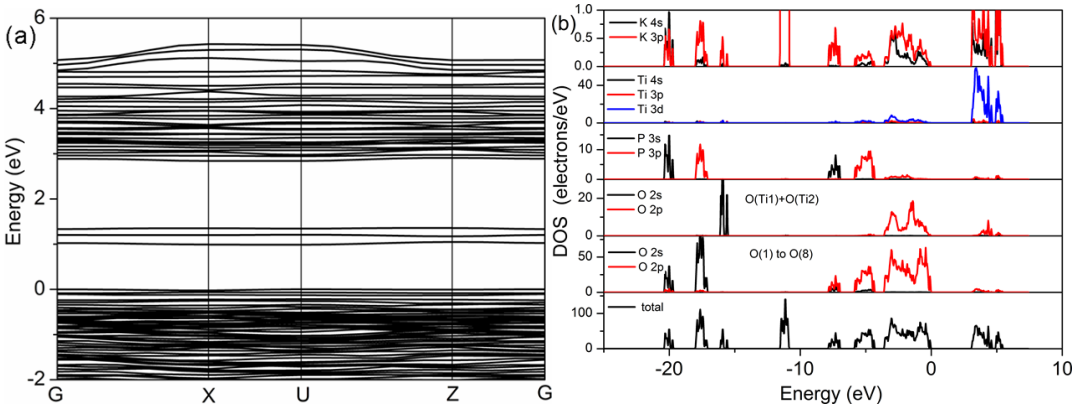

Fig. S11 (a) energy band structure and (b) the total density of states (TDOS) and partial density of states (PDOS) in KTP with three oxygen vacancies from O(1) to O(8) in a unit cell.

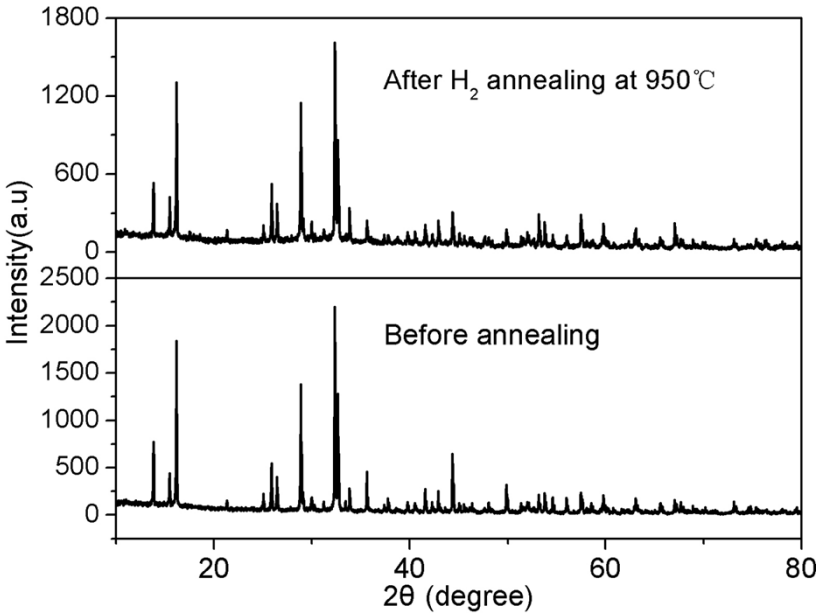

Fig. S12 X-ray powder diffraction patterns of KTP before and after H_2 annealing. The hydrogen annealing process at 950 °C did not induce a phase transition.

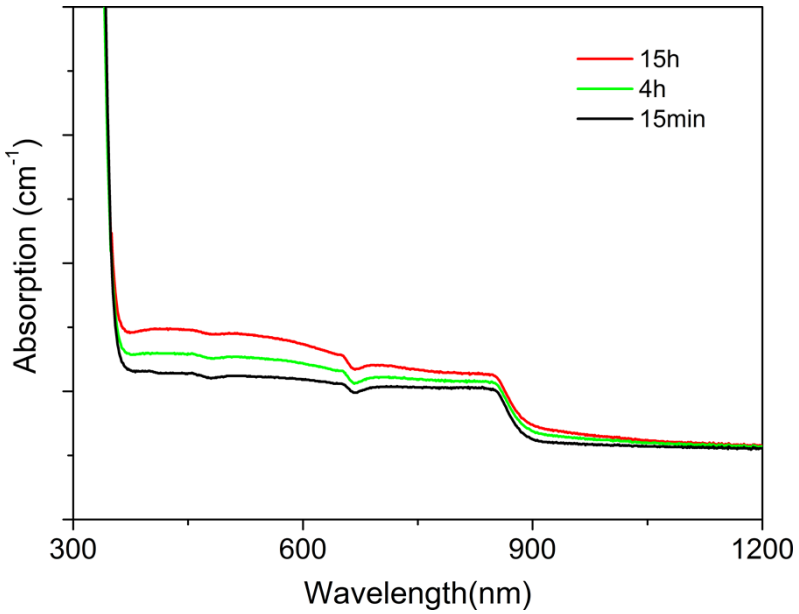

Fig. S13 Experimental absorption spectra of KTP with different annealing times (600 °C, H_2:N_2=1:8).

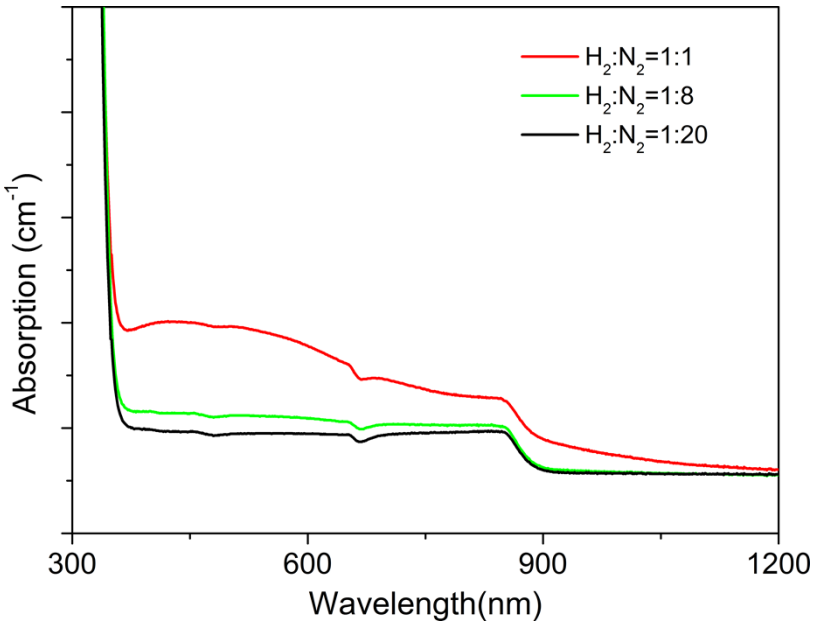

Fig. S14 Experimental absorption spectra of KTP with different hydrogen concentration (600 °C, 4h).

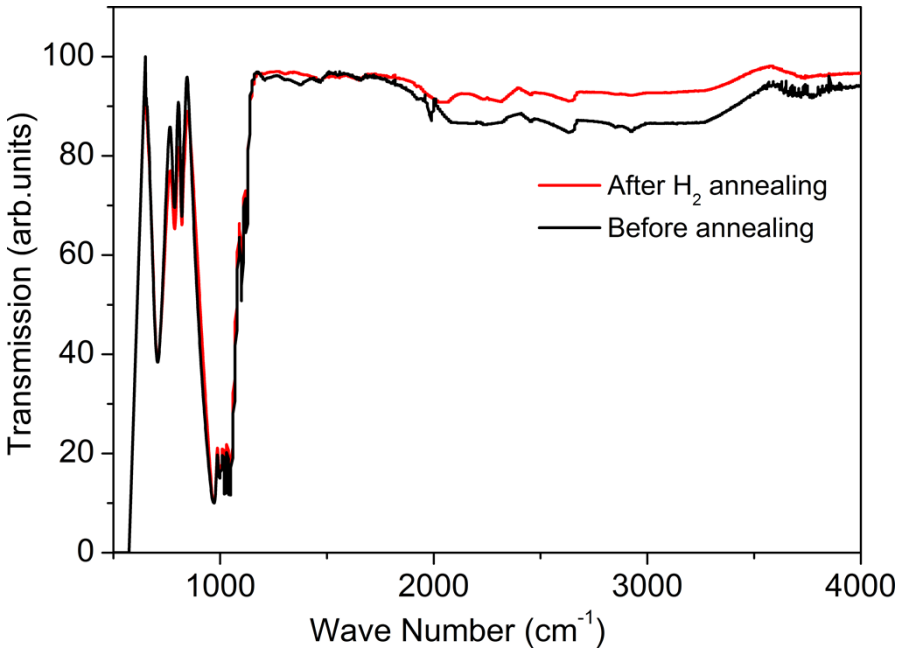

Fig. S15 Infrared spectra of KTP before and after hydrogen annealing at 950 °C. There is no absorption peak of H_2O observed after hydrogen annealing.

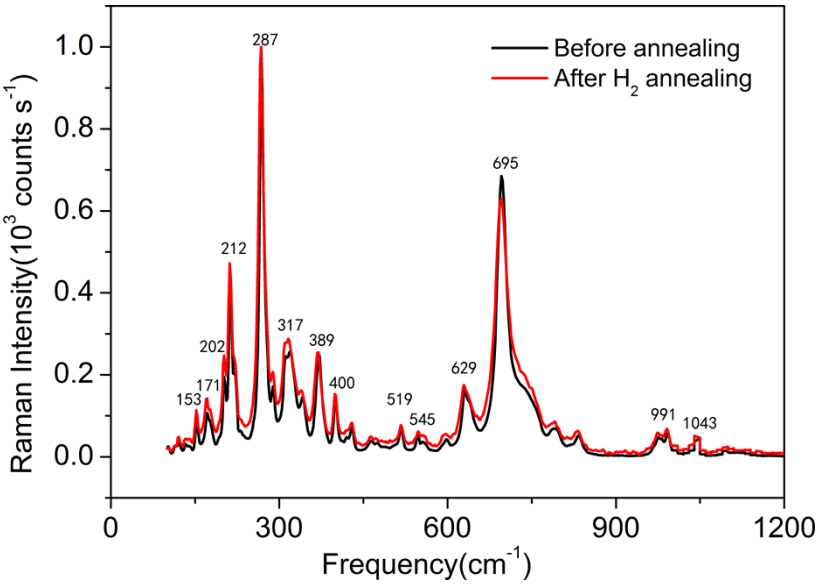

Fig. S16 Raman spectra of KTP before and after hydrogen annealing at 950 °C. There is no vibration mode of H_2O in the Raman spectrum after hydrogen annealing.

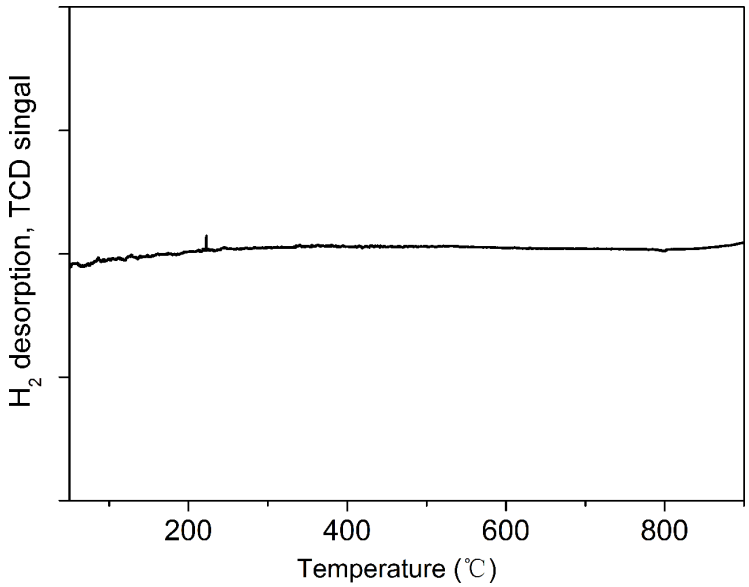

Fig. S17 H_2-temperature programmed desorption (H_2-TPD) profile of KTP from room temperature to 900 °C.

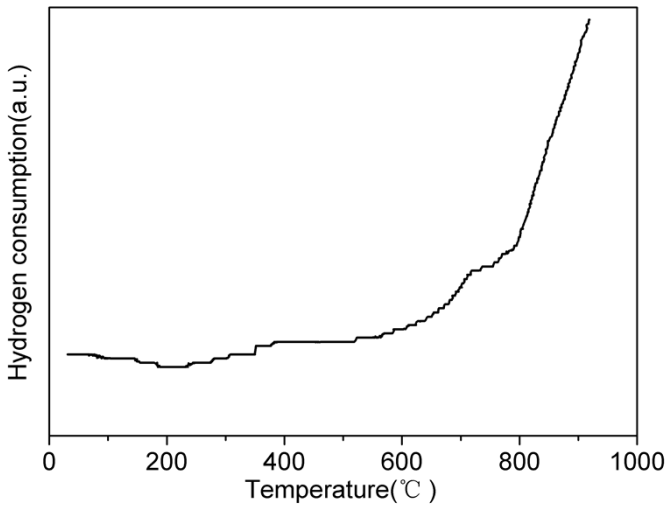

Fig. S18 H_2-temperature-programmed reduction (H_2-TPR) profile of KTP from room temperature to 900 °C.

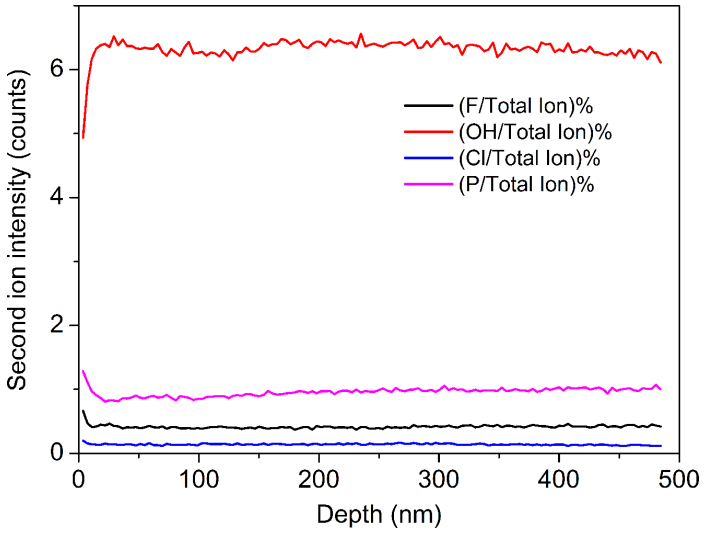

Fig. S19 Secondary ion mass spectroscopy (SIMS) of KTP after hydrogen annealing at 950 °C.